

Analysis of flows of ferrofluids under simple shear

Mark S. Korlie, Arup Mukherjee, Bogdan G. Nita, John G. Stevens, A. David Trubatch and Philip Yecko

Department of Mathematical Sciences, Montclair State University, 1 Normal Avenue, Montclair, NJ 07043, USA

E-mail: mukherjee@mail.montclair.edu

Abstract.

We analyze the nature of steady solutions of a sheared ferrofluid between two parallel boundaries and subject to an applied magnetic field \mathbf{H} perpendicular to the boundaries. Making no *a priori* assumption about the magnitude of spin, we find solutions numerically for the velocity and spin fields under combined pressure gradient and boundary flow forcing. The numerical technique is valid for arbitrary spin viscosity and by approaching asymptotically small values we explore the impact of the spin boundary conditions on the flow. When the imposed magnetic field is time independent its effect on the flow is dissipative but spatially varying fields still permit control of the velocity profile, including the breaking of its midplane symmetry. Time dependent or rotating perpendicular fields can drive the flow and allow more complete flow control, as illustrated in a simple numerical experiment that approximates plug flow.

1. Introduction

There is broad interest in sheared flows of ferrofluids subject to various forms of magnetic forcing. Early work focused on the spin-up problem and on traditional applications, such as ferrofluid seals and heat transfer devices. Recent attention is on the possibilities to control fluid within micro-electro-mechanical systems (MEMS) and nanoscale devices.

Studies by Zahn and colleagues [4, 9, 10] have examined simple sheared ferrofluids forced by time dependent magnetic fields under the assumption of small spin velocity and creeping flow. More recent work [2, 3] has relaxed the small spin velocity assumption and considered steady driving, but is restricted to zero spin viscosity and plane Couette creeping flows (linear velocity profiles).

In this study, we adopt a channel geometry, where the ferrofluid is confined between two infinite parallel plates, flowing with a simple shear (or Couette-Poiseuille) velocity profile. We assume creeping flow, although doing so is not strictly necessary because inertial effects are automatically neglected for steady simple shears. In addition, we maintain the presence of antisymmetric stresses and effects of spin viscosity, although we make a number of other assumptions, as described in the next section. We primarily consider forcing by a magnetic field steady in time but spatially variable across the

channel. There is, however, greater practical interest in the effects of rotating or oscillatory fields. Since the resulting magnetic body force and couple are typically derived by time averaging, these terms are analogs of their steady counterparts. Based on this correspondence, we directly extend our analysis to include unsteady driving effects.

2. Governing equations

We consider a ferrofluid between two parallel plates separated by a distance d as shown in figure 1. A steady magnetic field \mathbf{H} is applied transverse to the sample along the x -axis. The governing equations are the momentum and angular momentum balance equations and the magnetization equation [1, 4, 5, 6, 7, 8]

$$\rho \left(\frac{\partial \mathbf{u}}{\partial t} + \mathbf{u} \cdot \nabla \mathbf{u} \right) = \nabla \cdot \mathbb{T} + \mathbf{f} \quad (1)$$

$$\rho I \left(\frac{\partial \boldsymbol{\omega}}{\partial t} + \mathbf{u} \cdot \nabla \boldsymbol{\omega} \right) = \nabla \cdot \mathbb{C} + \mathbf{T} + \mathbf{L} \quad (2)$$

$$\frac{\partial \mathbf{M}}{\partial t} + \mathbf{u} \cdot \nabla \mathbf{M} = \boldsymbol{\omega} \times \mathbf{M} - \frac{1}{\tau} (\mathbf{M} - \mathbf{M}_0), \quad (3)$$

where bold faced quantities represent vectors and the quantities \mathbb{T} and \mathbb{C} are tensors; I is the moment of inertia density; \mathbf{u} , the translational velocity; $\boldsymbol{\omega}$, the spin velocity of the suspension; \mathbf{M}_0 , the equilibrium magnetization; τ , the effective magnetization relaxation time and the other symbols have their usual meanings. For incompressible ferrofluids, the Cauchy stress tensor $\mathbb{T} = -p\mathbb{I} + \eta (\nabla \mathbf{u} + \nabla \mathbf{u}^T) + \zeta \mathbb{E} \cdot (\nabla \times \mathbf{u} - 2\boldsymbol{\omega})$, where η and ζ are the coefficients of shear and vortex viscosity, $\mathbf{T} = -\mathbb{E} : \mathbb{T}$ is the antisymmetric vector of the Cauchy stress; the couple stress tensor $\mathbb{C} = \eta' (\nabla \boldsymbol{\omega} + \nabla \boldsymbol{\omega}^T)$, where η' is the shear coefficient of spin viscosity; the body force density $\mathbf{f} = \mu_0 \mathbf{M} \cdot \nabla \mathbf{H}$, where μ_0 is the permeability of free space; and the body couple density $\mathbf{L} = \mu_0 \mathbf{M} \times \mathbf{H}$, the equilibrium magnetization for low magnetic fields is proportional to \mathbf{H} , $\mathbf{M}_0 = \chi \mathbf{H}$, with a constant of proportionality χ depending on temperature and the composition of the suspension. The magnetic flux \mathbf{B} is related to the magnetic field and magnetization by $\mathbf{B} = \mu_0 (\mathbf{H} + \mathbf{M})$. We assume that all field quantities are independent of y and z

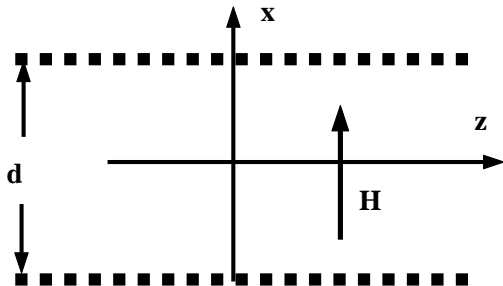


Figure 1. Planar ferrofluid layer between walls a distance d apart. Flow is driven by pressure gradient in the z direction and by shear of the upper plate and is magnetically stressed by a steady magnetic field \mathbf{H}

in the channel geometry with the exception of $\frac{\partial p}{\partial z}$ which can be a non-zero constant.

For the geometry in figure 1, the velocity $\mathbf{u} = (0, 0, U_z(x))$ and the spin velocity $\boldsymbol{\omega} = (0, \omega_y(x), 0)$. Moreover, Gauss's law for the magnetic flux and Ampere's law for the magnetic field in conjunction with zero jumps in the tangential component of \mathbf{H} and the normal component of \mathbf{B} yield $\mathbf{B} = (B_x, 0, B_z(x))$ and $\mathbf{H} = (H_x(x), 0, 0)$ where B_x is constant and $B_z(x) = \mu_0 M_z(x)$. We introduce dimensionless quantities by means of the following scalings: $\tilde{\mathbf{u}} = \mathbf{u}/U$, $\tilde{\mathbf{H}} = \mathbf{H}/H$, $\tilde{\mathbf{M}} = \mathbf{M}/H$, $\tilde{\boldsymbol{\omega}} = \boldsymbol{\omega}/\Omega$, $\tilde{p} = (d/U\eta)p$, and $\tilde{t} = (U/d)t$ for time, where the channel depth d also scales all lengths. From now on we work with the dimensionless variables, dropping all tildes ($\tilde{\cdot}$). With the additional scaling assumption that equates the (magnetization) relaxation, spin and fluid timescales: $\tau = 1/\Omega = d/U$, the magnetization equation (3) gives

$$M_x(x) = \frac{\chi H_x(x)}{1 + \omega_y(x)^2} \text{ and } M_z(x) = \frac{-\chi \omega_y(x) H_x(x)}{1 + \omega_y(x)^2}, \quad (4)$$

the linear momentum balance (1) reduces to

$$\left[1 + \frac{\zeta}{\eta}\right] \frac{d^2 U_z(x)}{dx^2} + 2 \left[\frac{\zeta}{\eta}\right] \frac{d\omega_y(x)}{dx} - \frac{\partial p}{\partial z} = 0 \quad (5)$$

and the balance of angular momentum (2) becomes

$$\epsilon \frac{d^2 \omega_y(x)}{dx^2} - 2 \frac{dU_z(x)}{dx} - 4\omega_y(x) - \chi \left[\frac{\mu_0 H^2}{\zeta \Omega}\right] \frac{H_x(x)^2 \omega_y(x)}{1 + \omega_y(x)^2} = 0, \quad (6)$$

where $\epsilon = \eta'/\zeta d^2$.

The dimensionless parameter ζ/η equals $3\phi/2$, where ϕ is the volume fraction of magnetic particles in the suspension, and the small parameter ϵ is proportional to the square of L_p/d , where L_p is the size of the magnetic particle. We choose $\mu_0 H^2/\zeta \Omega = O(1)$ to ensure that the effect of the body couple, \mathbf{L} , is non-negligible. As observed by Rinaldi and Zahn [4], when ϵ is neglected, the combined effects of spin diffusion and spin/vorticity coupling results in boundary layers in $\boldsymbol{\omega}$ near walls and interfaces. In this case the boundary layers can have a significant effect on the shear stresses in these regions. In this paper, we solve the coupled second order differential equations (5) and (6) as boundary value problems on $x \in [0, 1]$ for the velocity fields $U_z(x)$ and $\omega_y(x)$ with ϵ small but non-zero for ferrofluid flows influenced by x -dependent magnetic fields $H_x(x)$ and driven by a combination of constant pressure gradient $\frac{\partial p}{\partial z}$ and a boundary shear. Appropriate boundary conditions on the velocity $U_z(x)$ and spin velocity $\omega_y(x)$ are described in more detail in the next section.

3. Solution Method

Two point boundary value problems can be written in standard form as a first order system $\mathbf{y}'(x) = \mathbf{F}(x, \mathbf{y}(x))$ on $a \leq x \leq b$ with boundary conditions $\mathbf{g}(\mathbf{y}(a), \mathbf{y}(b)) = \mathbf{0}$ where \mathbf{y} , \mathbf{F} and \mathbf{g} have n (here 4) components and both \mathbf{F} and \mathbf{g} may be nonlinear. In this work we use MATLAB's *bvp4c* routine, a collocation based solver. Our use of *bvp4c* is standard except that we perform a continuation in successively smaller values ϵ in order to evaluate the limit as $\epsilon \rightarrow 0$.

Equations (5) and (6) are supplemented by the no-slip velocity conditions $U_z(0) = 0$ and $U_z(1) = V$ with V the speed of the upper plate, possibly zero. The spin velocity is required to satisfy the generalized boundary conditions $\omega_y(x) + aU_z(x) = b$ at $x = 0$ and $x = 1$, arising from fixing the antisymmetric part of the stress, or $2\boldsymbol{\omega} - \nabla \times \mathbf{u}$. The choice $a = \frac{1}{2}, b = 0$ corresponds to the vanishing of antisymmetric stress while $a = b = 0$ corresponds to a “spin no-slip” condition. In this work we adopt vanishing antisymmetric stress conditions.

4. Results

4.1. Constant field effects on pressure driven flows

In the spin inviscid limit, $\epsilon = 0$, equation (6) is reduced by two orders. Assuming spatially uniform $H_x(x)$, the resulting system can be solved exactly in two cases. In the first case, spin velocity is assumed to be of small magnitude and the pressure gradient dp/dz is assumed to be non-zero, but constant [4]. In this “small spin velocity” approximation, equation (6) becomes

$$-2\frac{dU_z(x)}{dx} - 4\omega_y(x) - \chi \left[\frac{\mu_0 H^2}{\zeta \Omega} \right] (H_x^2 \omega_y(x)) = 0. \quad (7)$$

Upon inspection of equation (7) together with equation (5) it becomes apparent that a linear $\omega_y(x)$ and quadratic $U_z(x)$ solves this system. In the second case, spin velocity is arbitrary but $dp/dz = 0$ [2, 3]. Inspection of equations (5) and (6) for $\epsilon = 0$ and $dp/dz = 0$ immediately reveals that the solution is a constant ω_y and linear $U_z(x)$.

Using the numerical method described above, we obtain solutions of (5) and (6) for constant dp/dz without a small spin velocity approximation and for arbitrary ϵ , including the limit $\epsilon \rightarrow 0$. In figure 2, we show the effect of decreasing values of ϵ for this pressure driven flow subject to constant magnetic field $H_x = 2$ with vanishing antisymmetric stress boundary conditions. When the spin velocity boundary layers are wide, the coupling between the magnetic forcing and the fluid is enhanced as can be seen in the modified velocity profiles U_z at all x . We observe that the vanishing antisymmetric stress boundary conditions correspond in this case to a source of vorticity at the walls and as a result the velocity profile is everywhere larger at the largest value of ϵ . Recalling that ϵ is proportional to the squared ratio of the magnetic particle size to channel width, we point out that values $\epsilon > 10^{-3}$ would be relevant only in nanochannels.

Note that the velocity curves (and to a lesser extent the spin) at $\epsilon = 10^{-3}$ and $\epsilon = 10^{-4}$ are almost indistinguishable in figure 2. We therefore choose $\epsilon = 10^{-4}$ to examine the effect of varying the magnitude of the uniform driving magnetic field in figure 3. In the absence of a magnetic field, a linear $\omega_y(x)$ solves equation (6); in this case $\boldsymbol{\omega} = \frac{1}{2}\nabla \times \mathbf{u}$ for all x , automatically satisfying the zero antisymmetric stress spin boundary conditions. For sufficiently large H , a linear $\omega_y(x)$ persists in the bulk of the channel. Notice that larger H diminishes the magnitude of the velocity throughout the channel. Indeed, for $H = 4$ the flux is reduced by 12% from the zero field case.

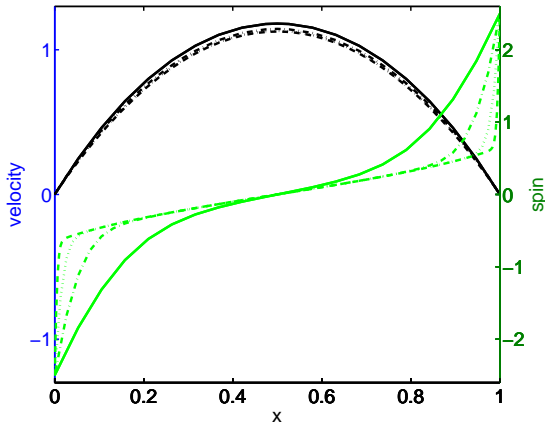


Figure 2. Effect of varying ϵ : velocity (black) and spin (green) with $\epsilon = 0.1$ (solid), $\epsilon = 0.01$ (dash-dot), $\epsilon = 10^{-3}$ (dotted) and $\epsilon = 10^{-4}$ (dashed); here $H = 2$ and $dp/dz = -10$.

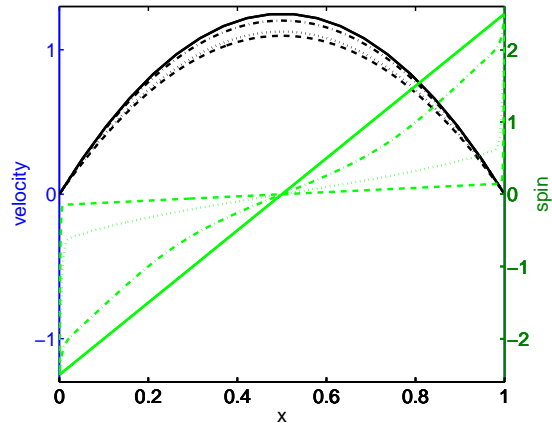


Figure 3. Effect of varying H : velocity (black) and spin (green) with $H = 0$ (solid), $H = 1$ (dash-dot), $H = 2$ (dotted) and $H = 4$ (dashed); here $\epsilon = 10^{-4}$ and $dp/dz = -10$.

4.2. Effect of shearing boundary conditions

To this point, we have considered driving the fluid only by pressure gradient. By also moving the upper wall in the z direction with velocity V , a *shearing boundary*, we can consider simple shear velocity profiles with pronounced asymmetry about the channel mid-plane. In figure 4 we present solutions for the velocity and spin fields for a range of upper wall velocities. It is clear that all of the spin profiles maintain a linear profile of the same slope throughout most of the channel, with thin boundary layers at each wall. Adding a moving upper wall to an ordinary pressure driven channel flow adds a linear component to the steady velocity field, and this effect dominates here, too, as apparent in figure 4. Zero antisymmetric stress boundary conditions on the spin require that the spin matches $-dU_z/dx$ at the walls. The vertical translation of the spin profiles observed in figure 4 is a direct consequence of changing the upper plate velocity V which produces an additive shift in the value of $-dU_z/dx$.

We next examine the impact of varying the imposed constant field H for a fixed non-zero upper plate velocity V . As seen in figure 5, larger values of the field dramatically alter the slope of the linear region of $\omega_y(x)$ (in agreement with the conclusion reached in the previous section with respect to figure 3). We again note that the largest H tends to produce smallest slope. In fact, as can be seen from equation (6), we must have $\omega_y \rightarrow 0$ as $H \rightarrow \infty$.

4.3. Spatially varying magnetic field

In the absence of a magnetic field, the velocity profile, $U_z(x)$, is symmetric with respect to the channel midpoint $x = 1/2$. For clarity, we introduce the shifted coordinate

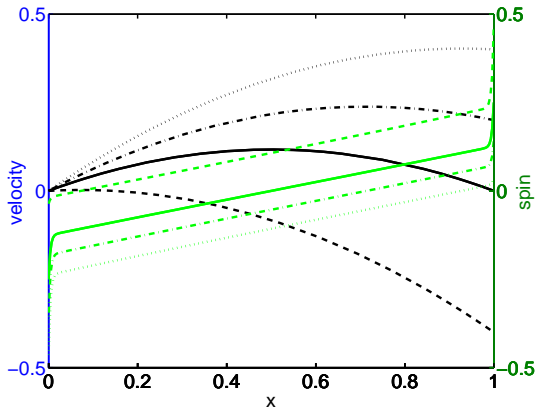


Figure 4. Effect of shearing boundary condition: $V = 0$ (solid), $V = 0.2$ (dash-dot), $V = 0.4$ (dotted) and $V = -0.4$ (dashed). Here $\epsilon = 10^{-4}$, $H = 2$ and $dp/dz = -1$.

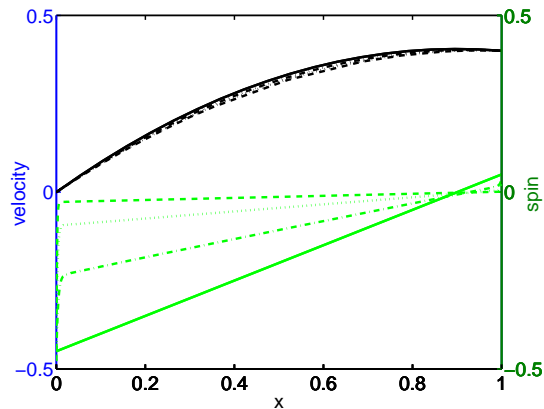


Figure 5. Effect of imposed field H with $V = 0.4$; $H = 0$ (solid), $H = 2$ (dash-dot), $H = 4$ (dotted) and $H = 8$ (dashed). Here $\epsilon = 10^{-4}$ and $dp/dz = -1$.

$\alpha = x - 1/2$ and refer to $U_z(\alpha)$ as an even function. The spin profile must therefore be an odd function by inspection of equation (5) since $d\omega_y/dx$ is required to be even. When a non-zero H field is present, these symmetries are maintained as long as $H_x(x)$ is symmetric (even), as can be directly verified from equation (6). In figures 6 and 7 we verify this property numerically for two driving pressure gradients: $dp/dz = -1$ and $dp/dz = -10$. The velocity profiles in figures 3 and 7 do not differ markedly from each other. The differences that we see in the spin profiles in figures 3 and 7 and are due to the specific nature of the imposed magnetic field. In figure 7 the spin velocity profiles have the same slope near the center of the channel. In fact this slope agrees with the slope of the solid curve corresponding to $H = 0$ in figure 3. We should not expect an asymmetric H to produce a symmetric spin profile. In fact, we see in figure 8 that this is the case: both $\omega_y(x)$ and $U_z(x)$ develop an observable asymmetry.

4.4. Time dependent magnetic fields

For the time independent imposed fields considered here, one is able only to increase the effective viscosity through a positive internal torque. However, as we have observed in section 4.3, it is possible to pump vorticity into the flow through the boundary layers. On the other hand, time dependent imposed fields could modify the internal torque, which will, in general, take on negative or complex character [4]. In this case, one could drive the flow selectively in x to achieve more desirable velocity profiles, such as plug flow; see figure 9 for an example.

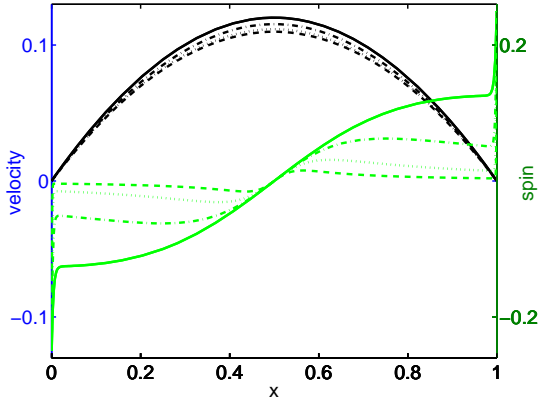


Figure 6. Imposed symmetric $H(x) = H_0(1/2 - x)$ for $H_0 = 2$ (solid), $H_0 = 4$ (dash-dot), $H_0 = 8$ (dotted) and $H_0 = 16$ (dashed). Here $dp/dz = -1$ and $\epsilon = 10^{-4}$.

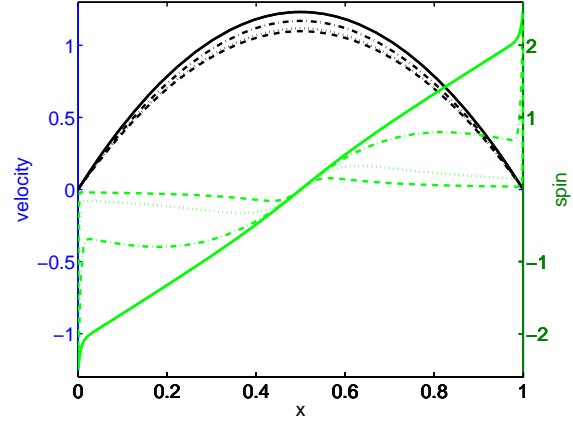


Figure 7. Imposed $H(x) = H_0(1/2 - x)$ for $H_0 = 2$ (solid), $H_0 = 4$ (dash-dot), $H_0 = 8$ (dotted) and $H_0 = 16$ (dotted). Here $dp/dz = -10$ and $\epsilon = 10^{-4}$.

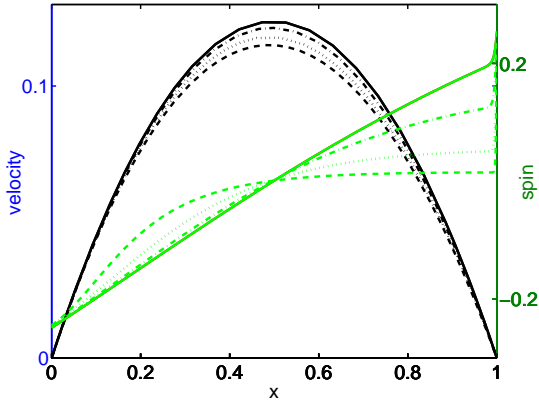


Figure 8. Imposed $H(x) = H_1x$ for $H_1 = 1$ (solid), $H_1 = 2$ (dash-dot), $H_1 = 4$ (dotted) and $H_1 = 8$ (dotted). Here $dp/dz = -1$ and $\epsilon = 10^{-4}$.

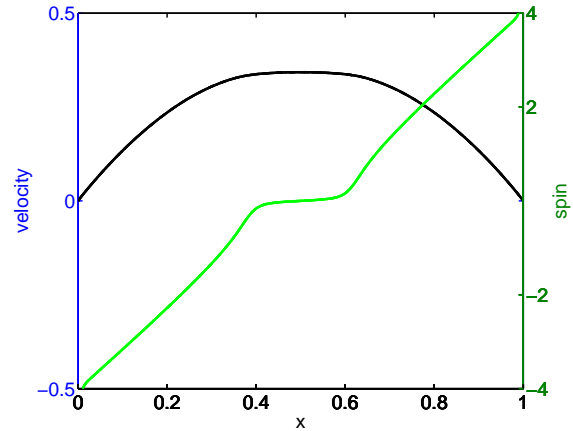


Figure 9. Imposed negative torque with $H(x) = 8i(1/2 - x)$. Here $dp/dz = -1$ and $\epsilon = 10^{-4}$.

5. Summary and discussion

We have used a robust numerical method to find steady solutions for the velocity and spin fields of a ferrofluid shear flow in the limit of small but non-vanishing spin viscosity. Although derived in the creeping flow limit, the steady solutions are valid for parallel flow at any finite Reynolds number and do not assume a “small spin velocity”. We maintain zero antisymmetric stress boundary conditions, which can be interpreted as fixing the spin to match $-dU/dx$ at $x = 0$ and $x = 1$. Constant imposed magnetic fields lead to essentially linear spin fields and near quadratic (Poiseuille) velocity fields

with larger fields reducing the slope of the linear region of the spin field. The spin viscosity determines the width of the spin boundary layer and consequently the extent to which the spin solution is essentially linear. Departures from linear spin profiles in the bulk of the flow couple to and therefore modify the velocity profile solution. Thus, the effect of spin boundary conditions should be directly observable in nanochannel flow profiles. These effects have been examined from a different perspective by examining the complementary case of shearing boundary conditions.

Time independent magnetic fields have an effect that depends on their symmetry: spatially linear fields symmetric about the channel midpoint produce symmetric spin and velocity solutions, although these are no longer linear and quadratic, respectively. Asymmetric magnetic fields produced asymmetric spin and velocity solutions, but the effect on the velocity was small.

There are several interesting areas for future study. We intend first to perform a complete linear stability analysis of ferrofluid channel flows. There is the intriguing possibility that creeping flows may be destabilized by a magnetic field. While intrinsically stable by itself, creeping flow has been found to become unstable in the presence of other effects, such as an interface.

References

- [1] Felderhof B U 2000 *Phys. Rev. E* **62(3)** 3848
- [2] He X, Elborai S, Kim D, Lee S H and Zahn M 2005 *J. App. Phys.* **97** 10Q302
- [3] Rhodes S, He X, Elborai S, Lee S H and Zahn M 2006 *J. Electrostatics.* **64** 513
- [4] Rinaldi C and Zahn M *Phys. Fluids* **14(8)** 2847
- [5] Rosensweig R E 1997 *Ferrohydrodynamics* Dover
- [6] Rosensweig R E 2000 *Magnetohydrodynamics* **36(4)** 303
- [7] Rosensweig R E 2004 *J. Chem. Phys.* **10** 1228
- [8] Shliomis M I 2002 *Lecture Notes in Physics 594* Springer-Verlag 85
- [9] Zahn M and Greer R G 1995 *J. Magn. Magn. Mater.* **149** 165
- [10] Zahn M and Pioch L L 1999 *J. Magn. Magn. Mater.* **201** 144